Published in final edited form as:
*Hypertension*. 2014 September ; 64(3): 541–550. doi:10.1161/HYPERTENSIONAHA.114.03549.

# HV1 ACTS AS A SODIUM SENSOR AND PROMOTES SUPEROXIDE PRODUCTION IN MEDULLARY THICK ASCENDING LIMB OF DAHL SALT-SENSITIVE RATS

**Chunhua Jin**[1], **Jingping Sun**[1], **Carly A. Stilphen**[1], **Susan M. E. Smith**[4], **Hiram Ocasio**[1], **Brent Bermingham**[1], **Sandip Darji**[1], **Avirup Guha**[1], **Roshan Patel**[1], **Aron M. Geurts**[3], **Howard J. Jacob**[3], **Nevin A. Lambert**[2], and **Paul M. O'Connor**[1]

[1]Department of Physiology, Georgia Regents University, Augusta, GA, USA

[2]Department of Pharmacology and Toxicology, Georgia Regents University, Augusta, GA, USA

[3]Department of Physiology, Medical College of Wisconsin, Milwaukee, WI, USA

[4]Department of Biology & Physics Kennesaw State University, Atlanta, GA

## Abstract

We previously characterized a $H^+$ transport pathway in medullary thick ascending limb nephron segments that when activated stimulated the production of superoxide by NAD(P)H oxidase. Importantly, the activity of this pathway was greater in Dahl salt-sensitive rats than salt-resistant ($SS.13^{BN}$) rats, and superoxide production was enhanced in low $Na^+$ media. The goal of this study was to determine the molecular identity of this pathway and its relationship to $Na^+$. We hypothesized that the voltage-gated proton channel, HV1, was the source of superoxide-stimulating $H^+$ currents. In order to test this hypothesis, we developed $HV1^{-/-}$ null mutant rats on the Dahl salt-sensitive rat genetic background using zinc-finger nuclease gene targeting. HV1 could be detected in medullary thick limb from wild-type rats. Intracellular acidification using an $NH_4Cl$ prepulse in 0 sodium/$BaCl_2$ containing media resulted in superoxide production in thick limb from wild-type but not $HV1^{-/-}$ rats ($P<0.05$), and more rapid recovery of intracellular pH in wild-type rats (ΔpHi 0.005U/sec vs. 0.002U/sec, $p=0.046$ respectively). Superoxide production was enhanced by low intracellular sodium (<10mM) in both thick limb and peritoneal macrophages only when HV1 was present. When fed a high salt diet, blood pressure, outer-medullary renal injury (tubular casts) and oxidative stress (4-Hydroxynonenal staining) were significantly reduced in $HV1^{-/-}$ rats compared to wild-type Dahl salt-sensitive rats. We conclude that HV1 is expressed in medullary thick ascending limb and promotes superoxide production in this segment when intracellular $Na^+$ is low. HV1 contributes to the development of hypertension and renal disease in Dahl salt-sensitive rats.

**CORRESPONDING AUTHOR**: Dr. Paul O'Connor, Department Physiology, CB2206, Georgia Regents University, 1459 Laney-Walker Blvd, Augusta, GA, USA, 30912, Phone: 706 721 7890, Fax: 706 721 7661, paoconnor@gru.edu.

**Conflict(s) of Interest/Disclosure(s):**
None

**Keywords**

FREE RADICALS; HYPERTENSION; HVCN1; OXIDATIVE STRESS; PROTON CHANNEL

## Introduction

The Dahl salt-sensitive (SS) rat is a naturally occurring model of salt-sensitive hypertension that closely mimics human forms of disease observed in the African American population [1–6]. A number of previous studies indicate that oxidative stress, specifically within the renal outer medullary region, promotes the development of hypertension and renal injury in the SS rat model [6–8]. Within this region, renal medullary thick ascending limb tubular segments (mTAL) are thought to be the greatest source of reactive oxygen species and much of the superoxide produced by this segment is derived from NAD(P)H oxidase [9]. As we have shown superoxide production is enhanced in mTAL of SS rats compared to salt-resistant animals [10–12], it is likely that superoxide production by this segment contributes to the development of disease in these animals. The cellular mechanisms responsible for augmented superoxide production in mTAL of salt-sensitive rats when fed a high salt diet however, remain unclear.

Superoxide production in mTAL in response to cellular $H^+$ efflux was initially reported by Li et al [13]. We have since characterized a novel $H^+$ transport pathway in mTAL, that when activated stimulated the production of superoxide by NAD(P)H oxidase [10]. Importantly this pathway was enhanced in SS rats compared to salt-resistant control animals ($SS.13^{BN}$)[10]. A number of indicators suggested that HV1, a voltage-gated $H^+$ channel expressed highly in immune cells [14], could be the unidentified $H^+$ transport pathway we characterized in mTAL. First, as charged protons cannot readily cross the plasma membrane [15] we suspected an ion channel. Second, superoxide production was only observed in the presence of a large outward pH gradient, not following an inward pH gradient [10]. Third, proton efflux was linked to cellular depolarization and activation of the NAD(P)H oxidase [10]. HV1 fulfilled all these criteria. HV1 is specific to protons [15]. The opening of HV1 is pH dependent with the channel only mediating $H^+$ efflux, not influx, under physiological conditions [15, 16]. HV1 opening is voltage-dependent, opening in response to cellular depolarization, and HV1 has been associated with NADPH oxidase [15, 17, 18].

Given the number of characteristics shared between HV1 and the unidentified $H^+$ transport pathway we characterized in mTAL, we hypothesized that ‘HV1 is present in mTAL and contributes to superoxide producing $H^+$ currents following cellular acidification. Further, as high salt feeding is likely to promote both depolarization as well as acidification of mTAL secondary to enhanced apical Na reabsorption [19, 20] and increased acid delivery to this segment [21, 22], (factors we predict would promote opening of HV1 *in vivo*) we hypothesized that ‘activation of Hv1 contributes to the development of outer-medullary oxidative stress, hypertension and renal injury *in vivo* following high salt feeding in Dahl salt-sensitive rats’. As, specific pharmacological inhibitors of HV1 are not yet available[23], we tested this hypothesis by developing an $HV1^{-/-}$ null mutant rat on the Dahl salt-sensitive rat (Medical College of Wisconsin) genetic background.

As our previous work indicated reactive oxygen species (ROS) production in response to $H^+$ efflux was greatly enhanced by low extracellular $Na^+$ [10], we also investigated the relationship between Na concentration, HV1 and NADPH oxidase activity in mTAL as alterations in Na handling could potentially be an important regulatory feedback system for ROS production in this segment[24–27].

## Methods

Studies used adult SS rats (Medical College of Wisconsin) maintained *ad libitum* on water and a standard pellet diet containing 0.4% NaCl since weaning. All studies were conducted in accordance with the National Institutes of Health (NIH) Guide for the Care and Use of Laboratory Animals. All of the protocols were approved in advance by the institutional animal care committee at Georgia Regents University or the Medical college of Wisconsin.

### Bulk mTAL isolation

mTALs were isolated using a bulk dissection method as described previously [28] except two sieves rather than one were used. Briefly, the kidneys were flushed with 10ml of cold saline followed by 10ml of HEPES buffered Hanks Balanced salt solution (HBSS) containing 200 U/ml of type II collagenase (Worthington Biochemical). The kidneys were collected and cut into thin slices transversely along the cortical-medullary axis. The inner stripe of the outer medulla was isolated and incubated with collagenase solution at 37°C for 30minutes with intermittent pipetting. Every 5 mins, the digested tissue was pipetted out and passed through a 100μm and 70 μm sieve. mTAL segments were collected on the 70μm sieve, and digestion stopped by 1% BSA in pH 7.4 HBSS. We have previously demonstrated the collected tissue contains ~95% mTAL[29].

### Respiratory Burst Assay

Peritoneal macrophages (MØ) cells were collected as previously described [8]. In brief, rats were anesthetized with isoflurane (2–5%) and 50mL of HBSS was injected in to the abdominal cavity followed by a small midline incision. The excess fluid was collected by syringe. The collected fluids were centrifuged at 400 g for 10 min. Collected cell pellets which contain predominantly MØ [8] were resuspended and aliquoted onto a clear-bottom 96-well plate (Bioexpress) at ~$1*10^6$ cells per well. 1 mM L-012 (Wako Pharmaceuticals) was used to determine superoxide production using a FLUOstar Omega plate reader (BMG Labtech). Cells were maintained at 37°C and luminescence measured for 30 minutes at 2 minute intervals. Addition of 100μM of the PKC activator phorbol 12-myristate 13-acetate (PMA) was used to stimulate the respiratory burst and maximal luminescence (arbitrary units) recorded.

In order to set intracellular $Na^+$ concentration, cells were pre-incubated for 15min in solutions containing; 70mM N-methyl-D-glucamine, 5.5 mM D-glucose, 1.3mM $CaCl_2$, 1mM MgSO4, 5M HEPES at pH 7.4. NaCl levels were altered to maintain intracellular $[Na^+]$ ($[Na^+]_I$ at either 5, 10, 15, 20, or 25mM and balanced to a total of 70mM with the addition of KCl. The ionophore nystatin (135 U/mL) was prepared daily to permeablise cells to $Na^+$ [30]. In order to determine whether effects were due to differences in activity of Na/H

exchangers (NHE), 100μM of the NHE inhibitor cariporide was added. $ZnCl_2$ (100μM) was added to some wells to acutely inhibit HV1 activity. Maximal superoxide production rate was normalized to solutions containing 25mM NaCl within each plate.

### Transfection of Peritoneal Macrophages

Cells were obtained as above. After 2 h incubation, the cells were washed once with serum-free medium to eliminating non-adherent lymphocytes and polymorphonuclear leukocytes from the adherent macrophages, then cultured in 200 ul of 10% FBS DMEM supplemented with 500 U/ml rat Granulocyte Macrophage Colony Stimulating Factor (rGM-CSF) (GenScript, Cat# Z02992-10). The primary macrophages were cultured in the presence of rGM-CSF for 7 to 10 days prior to transfection.

hHvcn1 transfection: When the cells were reached 50–60% confluence, the medium was removed and 100 ul of fresh no pen/strep and no FBS DMEM added. For each well of 96 well plates, we diluted 150 ng of hHvcn1 (human Hvcn1 cDNA was cloned into pQBI25-fC3) into 7.5 ul of Opti-MEM (Gibco, Cat# 31985-062), with 0.3 ul of PromoFectin-Macrophage Transfection solution (PromoCell GmbH, Cat# PK-CT-2000-MAC-10). We then added PromoFectin-Macrophage solution to the DNA solution, vortex-mixed the solution and spun down briefly before incubating for 30 minutes at room temperature. We then added 15 ul of this mixture drop-wise into each well. After 4 hours incubation, we add 85 ul of no pen/strep 10% FBS DMEM to each well and put in a 37C incubator. After 48 hours of hHvcn1 transfection the respiratory burst assay was performed as detailed above.

### Micro dissection and imaging of mTAL

Rats were anesthetized with isoflurane (2–5%) and isolation of mTAL tissue strips performed as described previously[31]. Thin tissue strips containing mTALs were placed on a glass coverslip coated with the tissue adhesive Cell-Tak (BD Biosciences) for fluorescence imaging. Tissue strips containing mTALs were loaded with either dihydroethidium DHE (50 mmol/L) or 2',7'-Bis-(2-Carboxyethyl) -5-(And-6) - carboxyfluorescein (BCECF; 6 μmol/L) in HBSS for 1 hour at room temperature. Coverslips were placed on a heated imaging chamber maintained at 37°C (Warner Instruments) that allowed the rapid exchange of superfusion buffer and mounted on the stage of an inverted microscope (IX81 Olympus). mTAL were visualized with a ×40 water immersion objective lens. The signal was detected using a high-resolution digital camera (Photometrics Evolve, Roper Scientific). Excitation was provided by a Sutter DG-4 175W xenon arc lamp (Sutter Instruments) that allowed high-speed excitation wavelength switching. 3 to 10 mTAL epithelial cells were selected within each tissue strip to quantify changes in fluorescent intensity of dyes using Metafluor imaging software (Universal Imaging). Intracellular $[Na^+]$ was set at either 5 or 30mM using the same solutions as that used to set $[Na^+]_I$ in MØ.

### Whole cell voltage-clamp recordings

Proton currents from HV1 were recorded as previously described [32]. Traces shown in Figure 1 were not corrected for liquid junction potential, and leak currents were not subtracted.

### In vivo studies

Male 9 week male old WT SS and $HV1^{-/-}$ SS rats were anesthetized (2–5% isoflurane) and blood pressure telemeters (Data Sciences International, St Paul, MN) surgically implanted. Following 1 week of recovery, animals were again anesthetized and the left femoral vein catheterized for infusion of fluids. Surgically implanted catheters were then tunneled under the skin and exposed between the shoulder blades. Catheters were protected by a light wire spring attached to a swivel (Instech Laboratories Inc, Plymouth Meeting, PA), which allows free 360-degree movement of the animal. Rats were individually housed and allowed to recover for 1 week before beginning experimental measurements. Blood pressure was recorded 24 hr daily. Rats were initially be maintained on a low $Na^+$ (0.4% NaCl diet) before being switched to a 8% NaCl diet for 2 weeks. On day 3 of high NaCl feeding, rats were either maintained on vehicle infusions (1% DMSO in saline i.v. at a rate of 6.9 μL/min) of KR32568 (Sigma) added to the infusion media (2mg/Kg/day) to stimulate HV1. On day 15, rats were anesthetized and the kidneys excised for histological analysis. After processing, histological samples were blinded to the investigator and images quantified using Metamorph analysis software.

## Results

### Confirmation of HV1 deletion in mutant rats

HV1 mutant Dahl salt-sensitive rats were generated with zinc-finger nuclease technology (13, 16). Genomic DNA of homozygous HV1 mutant ($HV1^{-/-}$) rats was sequenced to reveal an 8 bp deletion, resulting in a frame-shift mutation and predicted loss of full length HVCN1 protein (Figure 1.a). Loss of HVCN1 was validated functionally using whole cell patch (Figure 1.b). Step changes in applied voltage between −60 + 100mV induced $H^+$ currents in 7 of 7 MØ cells from three wild-type rats while no current was observed in any of 9 cells studied from four $HV1^{-/-}$ mutant rats. These data are consistent with a single gene for HV1 and confirmed complete functional ablation in $HV1^{-/-}$ mutant rats. As HV1 is highly expressed in immune cells of the spleen and its localization known, we first confirmed the specificity of our mRNA primer and anti-HV1 antibody using whole spleen homogenates of Wild-type and $HV1^{-/-}$ mutant rats as *in situ* positive and negative controls, respectively. mRNA encoding HV1 was greatly reduced in spleen of $HV1^{-/-}$ mutant rats compared to wild-type rats (Figure 1.c). Western blot detected a band representing HV1 at the predicted molecular weight (32Kd) in the membrane fraction of spleen from wild-type but not $HV1^{-/-}$ mutant rats (Figure 1.d). Immunohistochemical staining of the spleen demonstrated numerous darkly stained cells within the spleen of wild-type rats, consistent with known distribution of HV1 in splenic tissue (Figure 1.e). HV1 protein staining was also nearly undetectable in whole cell homogenates of spleen from $HV1^{-/-}$ mutant rats compared to wild-type.

### HV1 expression in mTAL

In order to determine whether HV1 was expressed in mTAL of SS rats, we quantified mRNA and protein expression specifically in mTAL using the same PCR primers and antibodies used in spleen. mTAL from mutant rats served as a negative control. HV1 mRNA was 6 fold higher than presumed background in bulk isolated mTAL of wild-type compared

to $HV1^{-/-}$ mutant rats (please see http://hyper.ahajournals.org). We could not detect HV1 by Western in membrane fractions of bulk isolated mTAL in either genotype (data not shown); however, HV1 staining was identified specifically within mTAL in outer-medullary sections (Figure 2) and this was significantly greater than background staining in mTAL from mutant rats (4382±920AU vs 1458±709AU p=0.036, n=5). Anti-Hv1 immuno-gold staining and transmission electron microscopy localized Hv1 staining largely to the apical membrane of thick ascending limb (Figure 2).

### $H^+$ efflux mediated superoxide production in mTAL

In order to test our hypothesis that 'HV1 contributes to superoxide-enhancing $H^+$ currents in mTAL' we determined superoxide production (ΔEth/ΔDHE) in response to cellular acidification using an $NH_4Cl$ prepulse (20mM) under the conditions in which we previously used to characterize superoxide-stimulating $H^+$ currents [10]. Consistent with our previous work, superoxide production was stimulated following acidification in 0 $Na^+$, $BaCl_2$ (100μM) media in micro dissected mTAL from wild-type SS rats (Figure 3). In contrast, under the same conditions, cellular acidification with 20mM $NH_4Cl$ did not promote detectable changes in the rate of superoxide production in mTAL micro-dissected from $HV1^{-/-}$ mutant Dahl rats (Figure 3; $P_{STRAIN*TIME}<0.001$). Consistent with our hypothesis that $H^+$ efflux through HV1 promotes superoxide production in mTAL, intracellular pH ($[pH_I]$) recovery rate was significantly greater (p=0.046) and plateaued at higher $[pH_I]$ in mTAL from wild-type rats compared to $HV1^{-/-}$ mutant animals (slope = 0.005U/sec & 0.002U/sec; plateau= pH 7.35±0.29 vs. 7.08±0.04, respectively).

### HV1 and the $Na^+$ dependence of NAD(P)H oxidase in MØ

We next investigated the relationship between HV1, $Na^+$ concentration and NAD(P)H oxidase activity. In order to investigate this relationship in detail, we first utilized rat peritoneal MØ. These cells can be easily collected from the peritoneal cavity in large numbers, and express high levels of both HV1 and NAD(P)H oxidase. To determine whether changes in intracellular $Na^+$ concentration may have a direct effect on MØ superoxide production, intracellular $Na^+$ was set between (5–25mM) using the cation ionophore nystatin, and the NAD(P)H oxidase dependent respiratory burst was stimulated in MØ with PMA. Responses are shown normalized to the maximal response at 25mM $[Na]_I$ (Figure 4). We found that low $Na^+$ (5–10mM) greatly enhanced superoxide production in response to PMA (Figure 4; $P_{GROUP*SODIUM}=0.02$). The effect was due to intracellular $Na^+$, as no significant relationship with $Na^+$ was observed in the absence of the ionophore nystatin (Figure 4). Further, the effect was independent of Na/H exchange, as the relationship was maintained in the presence of the potent Na/H exchange inhibitor cariporide (Figure 4).

We measured superoxide production in MØ from HV1−/− mutant rats, and in MØ from WT rats in the presence of 100μM $Zn^{2+}$ (which acutely inhibits HV1 activity), to determine whether enhancement of NAD(P)H oxidase activity at low intracellular $Na^+$ is mediated by HV1. In cells from the same WT animal at 25mM $[Na^+]_I$, maximal raw signal was reduced from 4605±2006 arbitrary units (AU) in the absence of $Zn^{2+}$ to 1868±837AU in the presence of $Zn^{2+}$. In addition, no relationship between $[Na^+]$ and superoxide production was

observed in $Zn^{2+}$ treated MØ (Figure 4). Consistent with these data, no relationship between $[Na^+]_I$ and maximal superoxide production was observed during the respiratory burst in MØ harvested from $HV1^{-/-}$ mutant rats (Figure 4; raw signal at 25mM 5091±1551AU).

To determine whether the effect of Na on NAD(P)H oxidase depended on HV1 expression or was secondary to altered expression of other proteins during development, we transfected MØ harvested from $HV1^{-/-}$ mutant rats with human HV1. A significant relationship was observed between intracellular [Na] and PMA stimulated superoxide production in primary cultures of peritoneal MØ harvested from wild-type rats (Figure 5). Consistent with studies performed in freshly isolated MØ, this relationship was absent in cells from $HV1^{-/-}$ mutant rats (Figure 5). Transfection of MØ from $HV1^{-/-}$ mutant rats with human HV1 increased human HV1 expression ~2400 fold and restored the relationship between intracellular [Na] and superoxide production observed in wilt-type MØ (Figure 5). Apocyanin treatment (100μM) of WT cells diminished overall superoxide production (1513AU vs 126AU, for vehicle and apocynin treated primary cultured MØ at 25mM $[Na]_I$, respectively) and abolished the relationship between intracellular [Na] and superoxide production in wild-type cells (Figure 5), confirming superoxide production was mediated by NAD(P)H oxidase.

### Intracellular $Na^+$, HV1 and superoxide production in mTAL

To determine whether HV1 promotes superoxide in mTAL when intracellular $Na^+$ levels are low, we determined superoxide production (ΔEth/ΔDHE) in freshly micro-dissected live mTAL from wild-type and $HV1^{-/-}$ mutant rats at both 5mM and 30mM intracellular $[Na^+]$. In response to acidification using an $NH_4Cl$ (20mM) prepulse, the rate of superoxide production was enhanced in mTAL from wild-type rats at 5mM but not 30mM $[Na^+]_I$ (Figure 6; $P_{SODIUM*GROUP}<0.0001$). Importantly, in mTAL from $HV1^{-/-}$ mutant rats no significant difference was observed in superoxide production following acidification at either 5 or 30mM $Na^+$ (Figure 6).

24 hour mean arterial pressure measured by radio-telemetry was significantly lower in $HV1^{-/-}$ rats compared to wild-type animals following high salt feeding (8% NaCl) for 2 weeks ($P_{STRAIN}=0.046$). Outer-medullary tubular casts were markedly lower in $HV1^{-/-}$ rats compared to wild-type SS rats (Figure 7). Outer-medullary 4-HNE staining (oxidized lipids) was also markedly reduced in $HV1^{-/-}$ rats when compared to wild-type animals indicating reduced outer-medullary oxidative stress. Administration of KR32568 to activate HV1 *in vivo* did not alter blood pressure or outer-medullary injury markers. 4HNE staining tended to be elevated in KR32568 treated wild-type animals compared to vehicle, but this did not reach statistical significance (P=0.11).

## Discussion

HV1 is a voltage-gated proton channel highly expressed in immune cells where it acts to maintain NAD(P)H oxidase activity during the respiratory burst [14]. HV1 has been found in a number of cell types outside the immune system [23] including lung epithelial cells [33, 34] and spermatozoa [35]. However, no studies have identified the presence of HV1 in the mammalian kidney or have demonstrated a physiological link to ROS production in renal epithelial cells. This study demonstrates that HV1 is present in mTAL and that it contributes to $H^+$ efflux-

dependent superoxide production. Genetic deletion of HV1 in the SS rat was confirmed by sequence analysis revealing an 8-bp deletion in a key coding region of HV1. Complete functional knockout of the gene was confirmed by whole-cell voltage-clamp technique. Because murine gene knockout models have revealed lack of specificity of many commonly used antibodies [36], we first verified the specificity of a commercial antibody to HV1 *in situ* in spleen, a tissue in which HV1 expression is high and its localization known. Anti-HV1 from abcam (Cat# ab117520) clearly demonstrated expression of HV1 in spleen from WT but not from $HV1^{-/-}$ rats (Figure 1). When we used this antibody for Western blots, we found that detection depended on use of membrane fractions which are presumably enriched in HV1. Even in these enriched samples, the band for HV1 was weak, suggesting a limited sensitivity of this antibody for detection via Western blot. Immunohistochemical analysis of kidney sections using this antibody also detected HV1 (primarily around the apical membrane of thick ascending limb) in wild-type but not $HV1^{-/-}$ Dahl SS. The localization of HV1 to the apical membrane was also confirmed by transmission electron microscopy using immuno-gold stained sections. Although we were unable to detect HV1 protein expression in mTAL by western blot, the presence of HV1 in mTAL is supported by PCR, immunohistochemistry and functional analysis ($pH_I$).

Functional analysis of both superoxide production and $pH_I$ recovery following $NH_4Cl$ prepulse under the same conditions used to characterize superoxide-stimulating $H^+$ currents in our previous study (0 $Na^+$ media, $BaCl_2$)[10] demonstrate that HV1 is required for superoxide production following cellular acidification in mTAL [10]. Li *et al* first reported that stimulating $H^+$ efflux, either by rapidly increasing the pH of the extracellular media or by intracellular acidification using an $NH_4Cl$ prepulse promoted the production of superoxide by NAD(P)H oxidase in mTAL[13]. While Li et al concluded that any $H^+$ efflux promoted NAD(P)H oxidase activity including via Na/H exchangers, our own subsequent data did not support a direct link between Na/H exchanger activity and NAD(P)H oxidase activation. Instead, our data indicated that, in response to intracellular acidification, activation of a second unidentified $H^+$ transport pathway mediated superoxide production by the oxidase in this segment [10]. In both studies NADPH oxidase was confirmed as the source of $H^+$ efflux mediated ROS production using either apocynin or diphenylene iodonium [10, 13]. Our current data confirm our previous conclusions and identify this transport pathway as the voltage-gated proton channel HV1.

Another major finding of the current study is that HV1 modulates NAD(P)H oxidase activity in response to differing levels of intracellular [$Na^+$]. In our previous study we found that superoxide production following cellular acidification by $NH_4Cl$ was greatly enhanced in 0 $Na^+$ media [10]. In order to elucidate the relationship between $Na^+$, HV1 and NAD(P)H oxidase we first performed experiments in isolated peritoneal MØ from SS rats. MØ provided an excellent platform to investigate these relationships as they express high levels of HV1, can easily be isolated in large numbers, ROS production from NAD(P)H oxidase can be induced by addition of PMA and phagocytes are a well-established model to study the function of both HV1 and NAD(P)H oxidase [8, 37–39]. We found that low intracellular $Na^+$, between the ranges of 5–10mM, greatly enhanced ROS production during the PMA stimulated respiratory burst in MØ relative to 25mM $[Na^+]_I$. The effect was due to

intracellular $Na^+$ as in the absence of the ionophore nystatin, an increase in ROS production at low $Na^+$ levels was not observed. Importantly, the effect of low intracellular $Na^+$ to enhance maximal superoxide production in mTAL depended on the activity of HV1. In MØ from wild-type SS rats, addition of 100mM $Zn^{2+}$, which inhibits HV1, completely abolished the relationship between $Na^+$ and superoxide production. Further, in MØ isolated from $HV1^{-/-}$ rats no relationship between intracellular $Na^+$ and maximal superoxide production was observed unless these cells were transfected with human HV1 which restored the 'Na sensing' phenotype observed in wild-type cells. We conclude that HV1 must act to 'sense' intracellular $Na^+$ either directly or act as a signal to modulate the activity of NAD(P)H oxidase secondary to changes in intracellular $Na^+$. We confirmed these relationships in isolated mTAL from wild-type and $HV1^{-/-}$ rats using a second indicator of ROS production, dihydroethidium.

We and others have previously identified NADPH oxidase as the source of ROS following $H^+$ efflux in mTAL and we confirmed NADPH oxidase as the source of Na-sensitive superoxide production in MØ in the current study. Loss of 'Na sensing' was not due to loss of NAD(P)H oxidase activity as significant superoxide production was still detected in the absence of HV1. Further, expression of NADPH oxidase subunits was not altered between mTAL from wild-type and $HV1^{-/-}$ mutant rats (please see http://hyper.ahajournals.org) indicating systemic loss of HV1 did not alter NADPH oxidase expression in TAL during development. Our novel finding that HV1 acts to sense intracellular $Na^+$ and modulate NAD(P)H oxidase activity has broad implications to the study of the function of NAD(P)H oxidase activity in cells that express HV1.

Our finding that HV1 senses intracellular $Na^+$ and modulates NAD(P)H oxidase activity may be of particular relevance to mTAL in which changes in intracellular $Na^+$ are known to occur in response to alterations in $Na^+$ transport activity. Basal levels of intracellular $Na^+$ in mTAL have been reported between ~10–20mM, increase with the inhibition of Na/K/ATPase and decrease with inhibition of apical NKCC2 transporter activity [30, 40]. Importantly, based on our current data, we would predict that physiologically relevant changes in intracellular $Na^+$ of ± 5 to10mM from rest have the potential to markedly alter superoxide production via HV1 signaling. Given the important role of superoxide in stimulating the activity of $Na^+$ transporters in mTAL[41], $Na^+$ sensing by HV1 and subsequent alteration in local NAD(P)H oxidase activity may play an important role in the feedback regulation of $Na^+$ reabsorption by this segment.

While our study is the first to identify HV1 in mTAL, proton currents attributed to HV1 have previously been identified in proximal tubular cells of Frog (*Rana pippens*)[42]. In regard to their activation however, the authors of this study concluded that 'the role of depolarization activated $G_H$ (HV1) in proximal tubule is not entirely clear, since proximal tubule cells do not normally experience drastic changes in either pH or membrane potential'[42]. This brings into question the physiological relevance of HV1 in mTAL. While we observed functional effects attributed to HV1 in our studies, most of our experiments were performed under somewhat contrived conditions directed toward maximal activation and identification of the channel, including 0 $Na^+$, bicarbonate free media and rapid cellular acidification with $NH_4Cl$. What evidence is there then that HV1 would be activated in

mTAL under physiological conditions? Resting membrane potential in mTAL has been reported between −80mV to −40mV depending on transport conditions [19]. The trans-membrane voltage threshold for opening of HV1 can be described by $V_{threshold}$ = 20mV – 40ΔpH [33]. This voltage dependence is shifted −30 to −40mV during enhanced gating conditions associated with activation of NAD(P)H oxidase [15, 18]. Therefore, even under 'enhanced gating' conditions, in the absence of an outward pH gradient, HV1 within mTAL would remain in the closed state. Importantly, in regards to activation of HV1 in mTAL, a large outward pH gradient exists in this segment under normal physiological conditions. mTAL actively reabsorb much of the $NH_4^+$ secreted by the proximal tubule [43–45]. Due to the more rapid uptake of $NH_4^+$ across the apical membrane, and relatively slower loss of $NH_4^+$ relative to $NH_3$ across the basolateral membrane, under normal physiological conditions where the tubular perfusate contains ~4mM $NH_4^+$, an outward pH gradient of 0.8–0.9 units is present [43]. Such pH gradient would be predicted to result in a shift ~ 34mV toward more negative membrane potentials, within the range observed in mTAL. Therefore, due to the unique physiology of mTAL which results in a large outward pH gradient, we speculate that, even under normal physiological conditions, HV1 would be poised at or near its activated state. Differences in oxidative stress within the outer-medulla observed *in vivo* between wild-type and $HV1^{-/-}$ mutant rats further supports the concept HV1 in mTAL is active under physiological conditions (Figure 7).

Our *in vivo* data support a role of HV1 in the development of hypertension and kidney injury in Dahl SS rats. Blood pressure, was significantly lower in $HV1^{-/-}$ rats fed a high salt diet compared to wild-type SS rats, with HV1 accounting for about ~25% of the rise in arterial pressure. While this reduction in blood pressure is relatively modest, it is possible that it reflects a significant change in mTAL function. In regard to the final control of urinary Na excretion and blood pressure regulation, Na transport in mTAL is not thought to be as important as transport in more distal nephron segments. As evidence of this, heterozygous deletion of ROMK, which is critical for mTAL Na reabsorption, produces a relatively mild reduction in blood pressure in Dahl SS rats [46] similar to that observed in the current study following Hv1 deletion. In contrast, inhibition of epithelial Na channels in more distal nephron segments has a much greater effect [47]. A significant alteration in mTAL function is also consistent with our findings of marked reductions in outer-medullary oxidative stress and tubular injury, which were all more than 50% lower in $HV1^{-/-}$ animals and suggest an important role of HV1 in the development of tubulo-interstitial injury. Further studies are required to determine whether lower blood pressure in $HV1^{-/-}$ mutant rats is a consequence of altered mTAL function or related to other potential mediators of blood pressure such as immune cells which highly express Hv1 and have been demonstrated to be important in the development of hypertension in Dahl salt-sensitive rats[48].

Apical Na reabsorption is normally tightly coupled to basolateral NaKATPase activity, therefore despite enhancing Na transport, it is unlikely that a high salt diet would greatly alter intracellular [Na] in mTAL in the absence of other factors. Rather, as high NaCl delivery to the TAL promotes cellular depolarization secondary to increased NKCC2 activity [19, 20, 49], we speculate that HV1 may be activated by depolarization of the apical membrane. High salt diet has also been shown to increase acid excretion in Dahl SS rats[21]

which has been shown to promote both intracellular acidification [43] and cellular depolarization in mTAL secondary to low $pH_I$ inhibition of ROMK [22]. Therefore increased acid delivery to mTAL during high salt feeding may also promote opening of Hv1 *in vivo*.

As inhibition of Na/H exchangers has been demonstrated to activate HV1, we examined the effect of Na/H exchanger 1 (NHE) inhibition using KR32568 on *in vivo* responses to high NaCl diet in both wild-type and $HV1^{-/-}$ rats. *In vivo* administration of KR32568 during high NaCl feeding did not alter blood pressure or renal injury in either wild-type or $HV1^{-/-}$ rats and although oxidative stress (4HNE-staining) tended to be increased in wild-type animals, this did not reach significance. These data may suggest that either HV1 is already activated *in vivo*, or that greater activation of HV1 does not alter blood pressure/renal injury further. While our data confirm a role of HV1 in the development of hypertension and renal injury in Dahl SS rats, further studies are required to confirm whether this is mediated by mTAL HV1 expression or other sources such as circulating immune cells.

Current dogma holds that $H^+$ transport by HV1 allows NADPH to operate at a high rate by limiting cellular acidosis and depolarization which feedback upon activation of the oxidase to inhibit the enzyme [14]. A number of indicators suggest it is unlikely that superoxide production in mTAL would require $H^+$ efflux in order to prevent feedback inhibition of oxidase activity. Firstly, unlike phagocytic NADPH oxidase, which generates extracellular superoxide and requires $H^+$ efflux to balance the electron current, there is evidence epithelial NADPH oxidase generates largely intracellular superoxide and therefore would not require $H^+$ efflux across the cell membrane to balance charge [50, 51]. Secondly, superoxide production by NADPH oxidase in mTAL is much lower than that produced during the respiratory burst in phagocytes and significant cellular depolarization/acidification is not known to occur upon activation of the oxidase in these cells. An alternative explanation for our data is that, rather than solely preventing feedback inhibition of the oxidase, HV1 activation secondary to cellular depolarization in the presence of an outward pH gradient directly promotes the formation of superoxide by stimulating NADPH oxidase activity. Further studies will be required to resolve these key issues.

## Summary and Perspectives

In summary, we conclude that 1) HV1 is present in mTAL and contributes to superoxide production in response to $H^+$ efflux; 2) that HV1 modulates NADPH oxidase activity in response to the level of intracellular [$Na^+$]. 3) That HV1 contributes to the development of outer-medullary oxidative stress, hypertension and renal disease in high salt fed Dahl SS rats. This is the first functional evidence for a role of HV1 in the kidney and identifies HV1 as a potential target to limit renal oxidative stress and the development of salt-sensitive hypertension and renal injury. Our finding that HV1 regulates NAD(P)H oxidase activity in response to intracellular $Na^+$ levels may have important implications in regard to tubular $Na^+$ reabsorption and kidney function. This finding is also likely to have broad implications for other organ systems where HV1 is expressed. The development and characterization of a $HV1^{-/-}$ mutant rat model is likely to provide an important tool for the study of HV1 including its potential importance to cardiovascular disease.

## Supplementary Material

Refer to Web version on PubMed Central for supplementary material.

## Acknowledgments

The authors would like to thank the PhysGen KO program (http://rgd.mcw.edu/wg/physgenknockouts) for development of $HV1^{-/-}$ mutant rats. The authors would like to thank Kelly Hyndman for her careful review of the manuscript and the Electron Microscopy Core Services at Georgia Regents University.

**Source(s) of Funding:**

This work was supported by an American Heart Association Scientist Development Grant to Paul O'Connor (10SDG4150061), NIH GO grant RC2 HL101681 (Howard Jacob) and NIH GM078319 (Nevin Lambert).

## References

1. Sullivan JM. Salt sensitivity Definition, conception, methodology, and long-term issues. Hypertension. 1991; 17:I61–I68. [PubMed: 1987013]
2. Kotchen TA, Zhang HY, Covelli M, Blehschmidt N. Insulin resistance and blood pressure in dahl rats and in one-kidney, one-clip hypertensive rats. Am J Physiol. 1991; 261:E692–E697. [PubMed: 1767829]
3. Kidambi S, Kotchen JM, Krishnaswami S, Grim CE, Kotchen TA. Cardiovascular correlates of insulin resistance in normotensive and hypertensive african americans. Metabolism. 2010; 60:835–842. [PubMed: 20846700]
4. Bloch MJ, Basile J. African american patients with hypertensive chronic kidney disease receive no benefit on kidney disease progression from the currently recommended blood pressure goal of <130/80 mm hg unless there is significant proteinuria at baseline: Long-term follow-up of the aask study. J Clin Hypertens (Greenwich). 2011; 13:214–216. [PubMed: 21366854]
5. Campese VM. Salt sensitivity in hypertension Renal and cardiovascular implications. Hypertension. 1994; 23:531–550. [PubMed: 8144222]
6. Cowley AW Jr. Renal medullary oxidative stress, pressure-natriuresis, and hypertension. Hypertension. 2008; 52:777–786. [PubMed: 18852392]
7. Taylor NE, Glocka P, Liang M, Cowley AW Jr. Nadph oxidase in the renal medulla causes oxidative stress and contributes to salt-sensitive hypertension in dahl s rats. Hypertension. 2006; 47:692–698. [PubMed: 16505210]
8. Feng D, Yang C, Geurts AM, Kurth T, Liang M, Lazar J, Mattson DL, O'Connor PM, Cowley AW Jr. Increased expression of nad(p)h oxidase subunit p67(phox) in the renal medulla contributes to excess oxidative stress and salt-sensitive hypertension. Cell Metab. 2012; 15:201–208. [PubMed: 22326221]
9. Li N, Yi FX, Spurrier JL, Bobrowitz CA, Zou AP. Production of superoxide through nadh oxidase in thick ascending limb of henle's loop in rat kidney. Am J Physiol Renal Physiol. 2002; 282:F1111–F1119. [PubMed: 11997328]
10. O'Connor PM, Lu L, Liang M, Cowley AW Jr. A novel amiloride-sensitive h+ transport pathway mediates enhanced superoxide production in thick ascending limb of salt-sensitive rats, not na+/h+ exchange. Hypertension. 2009; 54:248–254. [PubMed: 19564541]
11. O'Connor PM, Lu L, Schreck C, Cowley AW Jr. Enhanced amiloride-sensitive superoxide production in renal medullary thick ascending limb of dahl salt-sensitive rats. Am J Physiol Renal Physiol. 2008; 295:F726–F733. [PubMed: 18579705]
12. Mori T, O'Connor PM, Abe M, Cowley AW Jr. Enhanced superoxide production in renal outer medulla of dahl salt-sensitive rats reduces nitric oxide tubular-vascular cross-talk. Hypertension. 2007; 49:1336–1341. [PubMed: 17470722]
13. Li N, Zhang G, Yi FX, Zou AP, Li PL. Activation of nad(p)h oxidase by outward movements of h + ions in renal medullary thick ascending limb of henle. Am J Physiol Renal Physiol. 2005; 289:F1048–F1056. [PubMed: 15972387]

14. DeCoursey TE. Voltage-gated proton channels find their dream job managing the respiratory burst in phagocytes. Physiology (Bethesda). 2010; 25:27–40. [PubMed: 20134026]
15. DeCoursey TE. Voltage-gated proton channels: Molecular biology, physiology, and pathophysiology of the h(v) family. Physiol Rev. 2013; 93:599–652. [PubMed: 23589829]
16. Musset B, Cherny VV, Morgan D, Okamura Y, Ramsey IS, Clapham DE, DeCoursey TE. Detailed comparison of expressed and native voltage-gated proton channel currents. J Physiol. 2008; 586:2477–2486. [PubMed: 18356202]
17. Musset B, Clark RA, DeCoursey TE, Petheo GL, Geiszt M, Chen Y, Cornell JE, Eddy CA, Brzyski RG, El Jamali A. Nox5 in human spermatozoa: Expression, function, and regulation. J Biol Chem. 2012; 287:9376–9388. [PubMed: 22291013]
18. DeCoursey TE, Cherny VV, Zhou W, Thomas LL. Simultaneous activation of nadph oxidase-related proton and electron currents in human neutrophils. Proc Natl Acad Sci U S A. 2000; 97:6885–6889. [PubMed: 10823889]
19. Schlatter E, Greger R. Camp increases the basolateral cl- -conductance in the isolated perfused medullary thick ascending limb of henle's loop of the mouse. Pflugers Arch. 1985; 405:367–376. [PubMed: 3001635]
20. Liu R, Garvin JL, Ren Y, Pagano PJ, Carretero OA. Depolarization of the macula densa induces superoxide production via nad(p)h oxidase. Am J Physiol Renal Physiol. 2007; 292:F1867–F1872. [PubMed: 17344185]
21. Batlle DC, Sharma AM, Alsheikha MW, Sobrero M, Saleh A, Gutterman C. Renal acid excretion and intracellular ph in salt-sensitive genetic hypertension. J Clin Invest. 1993; 91:2178–2184. [PubMed: 8486783]
22. Bleich M, Kottgen M, Schlatter E, Greger R. Effect of nh4+/nh3 on cytosolic ph and the k+ channels of freshly isolated cells from the thick ascending limb of henle's loop. Pflugers Arch. 1995; 429:345–354. [PubMed: 7761259]
23. Capasso M, DeCoursey TE, Dyer MJ. Ph regulation and beyond: Unanticipated functions for the voltage-gated proton channel, hvcn1. Trends Cell Biol. 2010; 21:20–28. [PubMed: 20961760]
24. Ortiz PA, Garvin JL. Superoxide stimulates nacl absorption by the thick ascending limb. Am J Physiol Renal Physiol. 2002; 283:F957–F962. [PubMed: 12372771]
25. Garvin JL, Ortiz PA. The role of reactive oxygen species in the regulation of tubular function. Acta Physiol Scand. 2003; 179:225–232. [PubMed: 14616238]
26. Juncos R, Garvin JL. Superoxide enhances na-k-2cl cotransporter activity in the thick ascending limb. Am J Physiol Renal Physiol. 2005; 288:F982–F987. [PubMed: 15821259]
27. Juncos R, Hong NJ, Garvin JL. Differential effects of superoxide on luminal and basolateral na+/h + exchange in the thick ascending limb. Am J Physiol Regul Integr Comp Physiol. 2006; 290:R79–R83. [PubMed: 16099821]
28. Trinh-Trang-Tan MM, Bouby N, Coutaud C, Bankir L. Quick isolation of rat medullary thick ascending limbs Enzymatic and metabolic characterization. Pflugers Arch. 1986; 407:228–234. [PubMed: 3018664]
29. Yang C, Stingo FC, Ahn KW, Liu P, Vannucci M, Laud PW, Skelton M, O'Connor P, Kurth T, Ryan RP, Moreno C, Tsaih SW, Patone G, Hummel O, Jacob HJ, Liang M, Cowley AW Jr. Increased proliferative cells in the medullary thick ascending limb of the loop of henle in the dahl salt-sensitive rat. Hypertension. 2012; 61:208–215. [PubMed: 23184381]
30. Ortiz PA, Hong NJ, Garvin JL. No decreases thick ascending limb chloride absorption by reducing na(+)-k(+)-2cl(−) cotransporter activity. Am J Physiol Renal Physiol. 2001; 281:F819–F825. [PubMed: 11592939]
31. Dickhout JG, Mori T, Cowley AW Jr. Tubulovascular nitric oxide crosstalk: Buffering of angiotensin ii-induced medullary vasoconstriction. Circ Res. 2002; 91:487–493. [PubMed: 12242266]
32. Ramsey IS, Ruchti E, Kaczmarek JS, Clapham DE. Hv1 proton channels are required for high-level nadph oxidase-dependent superoxide production during the phagocyte respiratory burst. Proc Natl Acad Sci U S A. 2009; 106:7642–7647. [PubMed: 19372380]

33. Cherny VV, Markin VS, DeCoursey TE. The voltage-activated hydrogen ion conductance in rat alveolar epithelial cells is determined by the ph gradient. J Gen Physiol. 1995; 105:861–896. [PubMed: 7561747]
34. Iovannisci D, Illek B, Fischer H. Function of the hvcn1 proton channel in airway epithelia and a naturally occurring mutation, m91t. J Gen Physiol. 2010; 136:35–46. [PubMed: 20548053]
35. Lishko PV, Kirichok Y. The role of hv1 and catsper channels in sperm activation. J Physiol. 2010; 588:4667–4672. [PubMed: 20679352]
36. Herrera M, Sparks MA, Alfonso-Pecchio AR, Harrison-Bernard LM, Coffman TM. Lack of specificity of commercial antibodies leads to misidentification of angiotensin type 1 receptor protein. Hypertension. 2012; 61:253–258. [PubMed: 23150519]
37. Morgan D, Capasso M, Musset B, Cherny VV, Rios E, Dyer MJ, DeCoursey TE. Voltage-gated proton channels maintain ph in human neutrophils during phagocytosis. Proc Natl Acad Sci U S A. 2009; 106:18022–18027. [PubMed: 19805063]
38. El Chemaly A, Okochi Y, Sasaki M, Arnaudeau S, Okamura Y, Demaurex N. Vsop/hv1 proton channels sustain calcium entry, neutrophil migration, and superoxide production by limiting cell depolarization and acidification. J Exp Med. 2009; 207:129–139. [PubMed: 20026664]
39. Kapus A, Romanek R, Qu AY, Rotstein OD, Grinstein S. A ph-sensitive and voltage-dependent proton conductance in the plasma membrane of macrophages. J Gen Physiol. 1993; 102:729–760. [PubMed: 8270911]
40. Yu M, Lopez B, Dos Santos EA, Falck JR, Roman RJ. Effects of 20-hete on na+ transport and na+ -k+ -atpase activity in the thick ascending loop of henle. Am J Physiol Regul Integr Comp Physiol. 2007; 292:R2400–R2405. [PubMed: 17303679]
41. Schreck C, O'Connor PM. Nad(p)h oxidase and renal epithelial ion transport. Am J Physiol Regul Integr Comp Physiol. 2011; 300:R1023–R1029. [PubMed: 21270341]
42. Gu X, Sackin H. Effect of ph on potassium and proton conductance in renal proximal tubule. Am J Physiol. 1995; 269:F289–F308. [PubMed: 7573477]
43. Watts BA 3rd, Good DW. Effects of ammonium on intracellular ph in rat medullary thick ascending limb: Mechanisms of apical membrane nh4+ transport. J Gen Physiol. 1994; 103:917–936. [PubMed: 8035168]
44. Attmane-Elakeb A, Karim Z, Bichara M. [role of the na(+)-k+(nh4+)-2cl cotransporter of the medullary ascending limb in the regulation of renal acid-base equilibrium]. Nephrologie. 2002; 23:209–211. [PubMed: 12227253]
45. Karim Z, Attmane-Elakeb A, Bichara M. Renal handling of nh4+ in relation to the control of acid-base balance by the kidney. J Nephrol. 2002; (15 Suppl 5):S128–S134. [PubMed: 12027211]
46. Zhou X, Zhang Z, Shin MK, Horwitz SB, Levorse JM, Zhu L, Sharif-Rodriguez W, Streltsov DY, Dajee M, Hernandez M, Pan Y, Urosevic-Price O, Wang L, Forrest G, Szeto D, Zhu Y, Cui Y, Michael B, Balogh LA, Welling PA, Wade JB, Roy S, Sullivan KA. Heterozygous disruption of renal outer medullary potassium channel in rats is associated with reduced blood pressure. Hypertension. 2013; 62:288–294. [PubMed: 23753405]
47. Pavlov TS, Levchenko V, O'Connor PM, Ilatovskaya DV, Palygin O, Mori T, Mattson DL, Sorokin A, Lombard JH, Cowley AW Jr, Staruschenko A. Deficiency of renal cortical egf increases enac activity and contributes to salt-sensitive hypertension. J Am Soc Nephrol. 2013; 24:1053–1062. [PubMed: 23599382]
48. Mattson DL, James L, Berdan EA, Meister CJ. Immune suppression attenuates hypertension and renal disease in the dahl salt-sensitive rat. Hypertension. 2006; 48:149–156. [PubMed: 16754791]
49. Haque MZ, Ares GR, Caceres PS, Ortiz PA. High salt differentially regulates surface nkcc2 expression in thick ascending limbs of dahl salt-sensitive and salt-resistant rats. Am J Physiol Renal Physiol. 2011; 300:F1096–F1104. [PubMed: 21307126]
50. Lassegue B, San Martin A, Griendling KK. Biochemistry, physiology, and pathophysiology of nadph oxidases in the cardiovascular system. Circ Res. 2012; 110:1364–1390. [PubMed: 22581922]
51. Li JM, Shah AM. Intracellular localization and preassembly of the nadph oxidase complex in cultured endothelial cells. J Biol Chem. 2002; 277:19952–19960. [PubMed: 11893732]

### Novelty and Significance: 1) What Is New 2) What Is Relevant? Summary

1. What is new? This study demonstrates that the voltage-gated proton channel HV1 is expressed in medullary thick ascending limb, that HV1 contributes to superoxide production in this segment, that HV1 acts to modulate superoxide production in response to changes in intracellular [$Na^+$] and that HV1 contributes to blood pressure regulation and renal injury in the Dahl salt-sensitive rat model.

2. What is Relevant? Superoxide production within the renal outer medulla by NAD(P)H oxidase is important in long-term blood pressure control and the development of renal injury via effects on $Na^+$ transport and renal hemodynamics and is augmented in Dahl salt-sensitive rats. We now identify HV1 as a critical component contributing to enhanced superoxide production in mTAL of Dahl salt-sensitive rats and a novel molecular target for the treatment of renal oxidative stress. Demonstration of HV1 as a $Na^+$ sensor, contributes to our understanding of the physiological stimuli that promote activation of NAD(P)H oxidase within the kidney and in other tissues expressing HV1.

In summary, we determined HV1 as the molecular identity of a source of superoxide in mTAL which is augmented in Dahl-salt-sensitive rats. Further, we demonstrate that HV1 acts to modulate the activity of NAD(P)H oxidase in both mTAL and MØ in response to physiologically relevant changes in intracellular $Na^+$ and that HV1 contributes to blood pressure regulation and renal injury in the Dahl salt-sensitive rat model. These data indicate that HV1 is likely to play an important physiological function as a $Na^+$ sensor and may provide a novel target for the treatment of renal oxidative stress, hypertension and kidney injury.

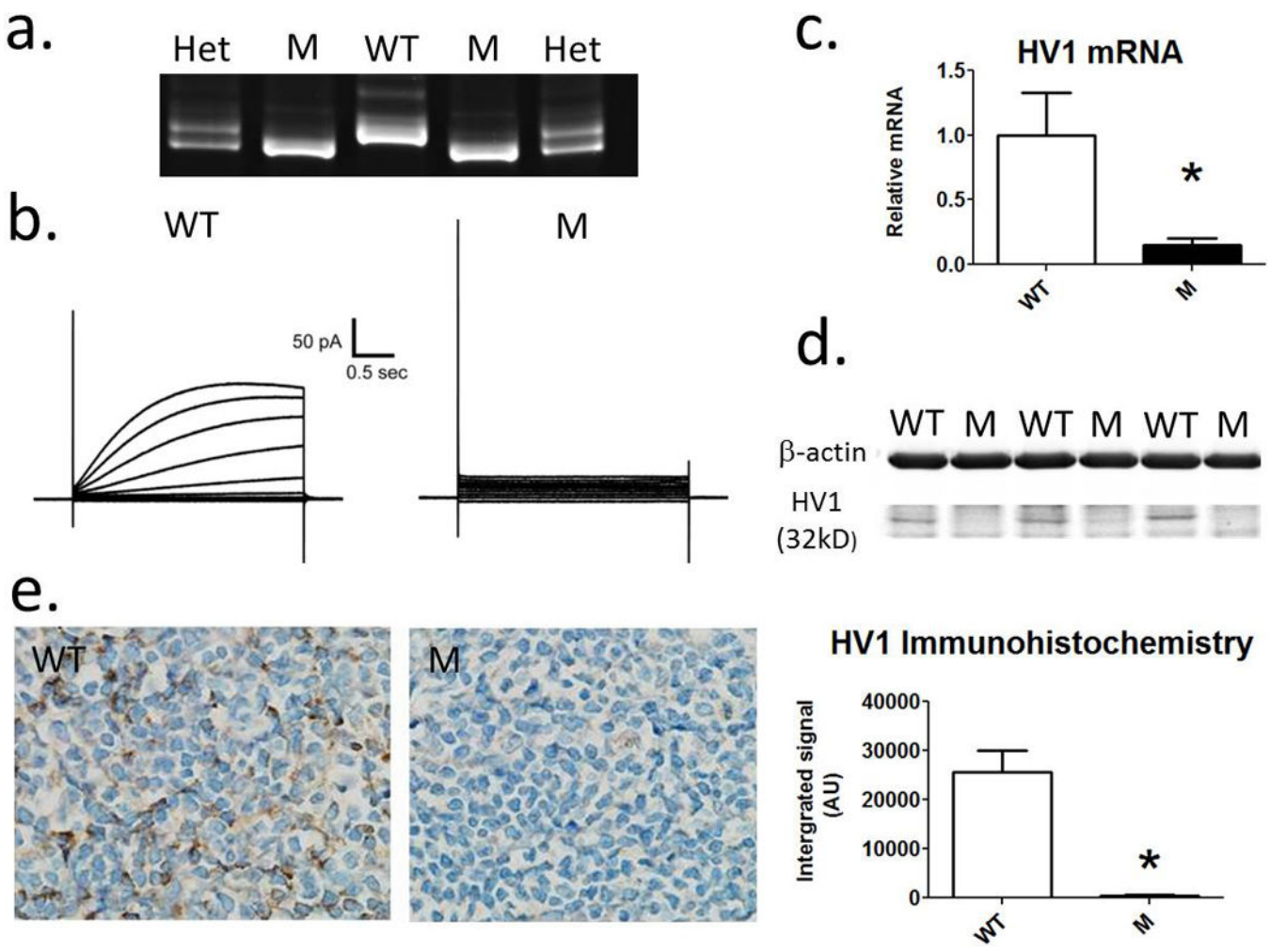


**Figure 1. Confirmation of loss of HV1 expression in mutant rats**

a) Representative gel for genotyping rats demonstrating 8bp deletion in gene encoding HV1. Lanes 1 and 5, heterozygous $HV1^{-/+}$ mutants (Het); lanes 2 and 3, homozygous $HV1^{-/-}$ Mutants (M); Lane 3, Wild-type (WT). b) A representative trace demonstrating proton currents in response to step changes in membrane potential in single peritoneal macrophages from wild-type (right) and mutant (left) rats. c) relative HV1 mRNA expression from spleen homogenates from WT (open columns) and M (closed columns) rats compared to GAPDH mRNA (n=4). d) Western blot for HV1 in membrane fraction of WT and M rats. A band representing HV1 is shown at ~32kd. e) Immunohistochemical staining of spleen using anti-HV1 in WT and M rats (n=4). Left, representative image of anti-HV1 stained tissue from WT and M rats at 40X. Right, quantification of anti-HV1 staining (integrated signal (arbitrary units (AU)). * = $p<0.05$ using unpaired t-test. Data are mean±SE.

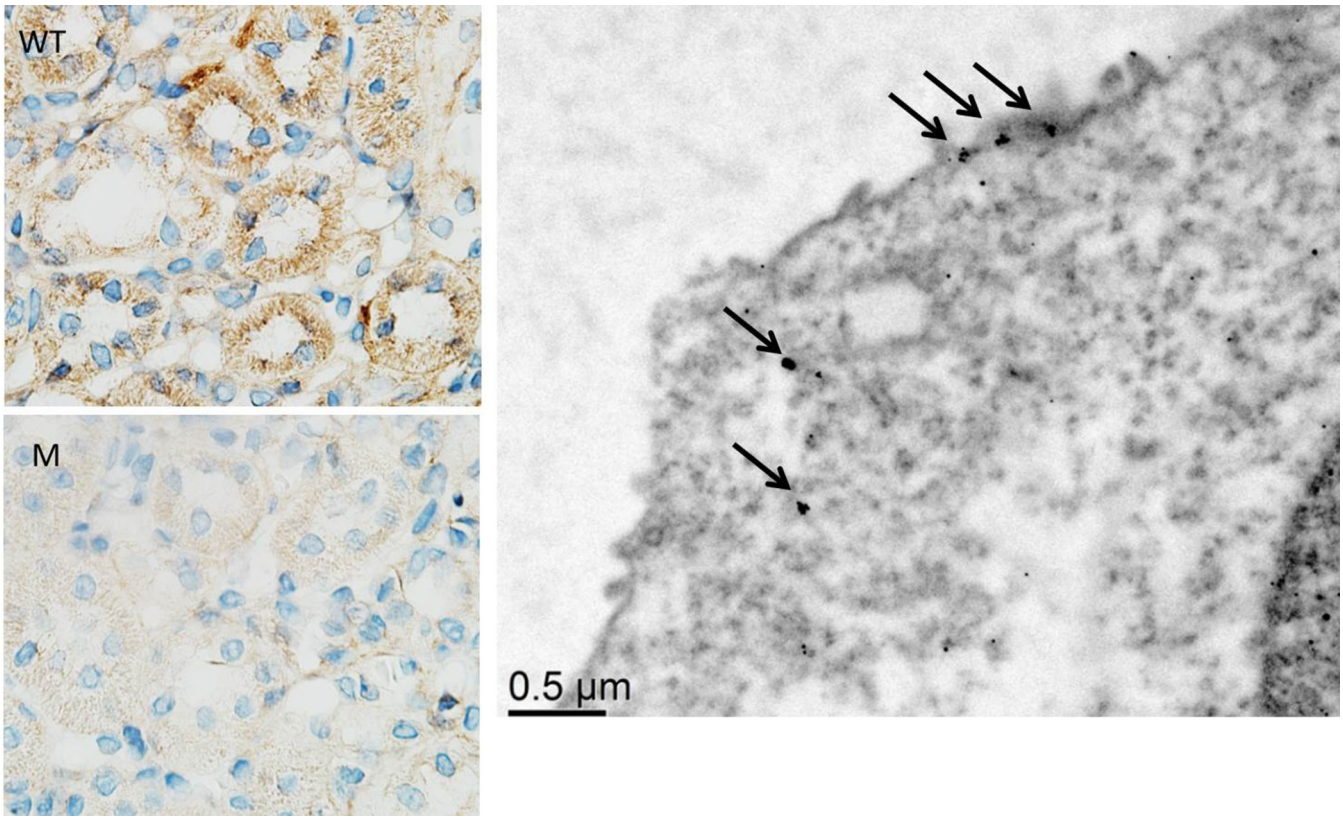


**Figure 2. HV1 expression in mTAL**

Legend does not match figure Left, representative immunohistochemical staining of renal outer medulla using anti-HV1 in WT and M rats at 100X magnification; Right, Electron micrograph demonstrating Hv1 localization to the apical membrane of renal medullary thick ascending limb cells using anti-HV1 immune-gold staining. Arrows indicate clumps of gold particles indicating HV1 expression.

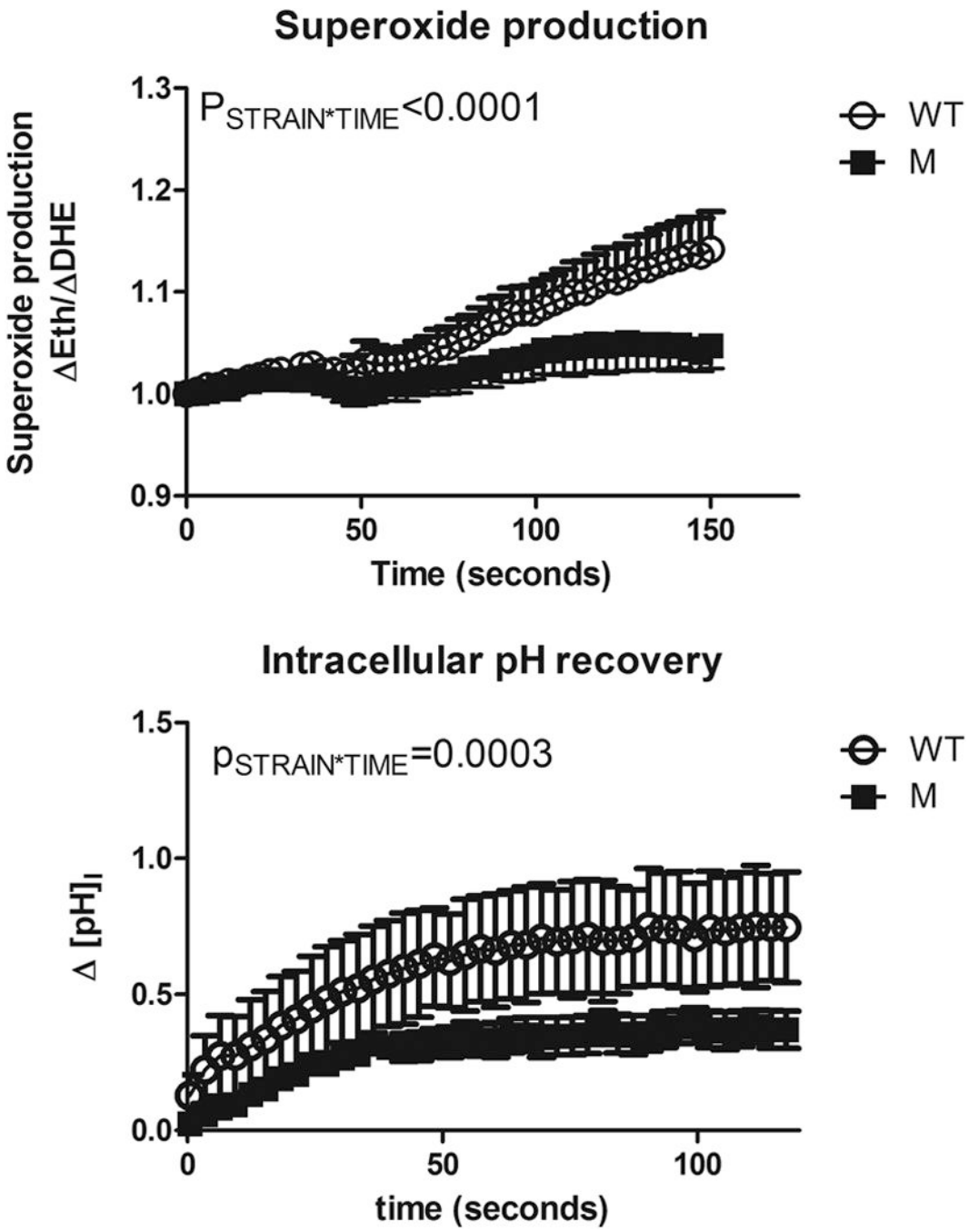


**Figure 3. Superoxide production and intracellular pH recovery in mTAL following $NH_4Cl$ prepulse**

(Top panel); superoxide production in isolated medullary thick ascending limb from wild-type (WT – open circles; n=6) and $HV1^{-/-}$ mutant (M – closed squares; n=7) rats loaded with the superoxide sensitive dye, dihydrethidium. × axis, time in seconds. $NH_4Cl$ (20mM) was removed from the bath at t=30 seconds. Y axis, superoxide production (ΔEth/ΔDHE) normalized to 1 at t=0. (Bottom panel); Intracellular pH recovery following removal of $NH_4Cl$ from the media in isolated medullary thick ascending limb WT (n=8) and M (n=6) rats. × axis, time in seconds following maximal acidification. y axis, change in intracellular

pH ($\Delta pH_I$) from maximal acidification. $P_{STRAIN*TIME}$, result of a two-way repeated measures ANOVA comparing response to WT and M rats. Media contained 0 $Na^+$, 100mM $BaCl_2$ (see methods). Data are mean±SE.

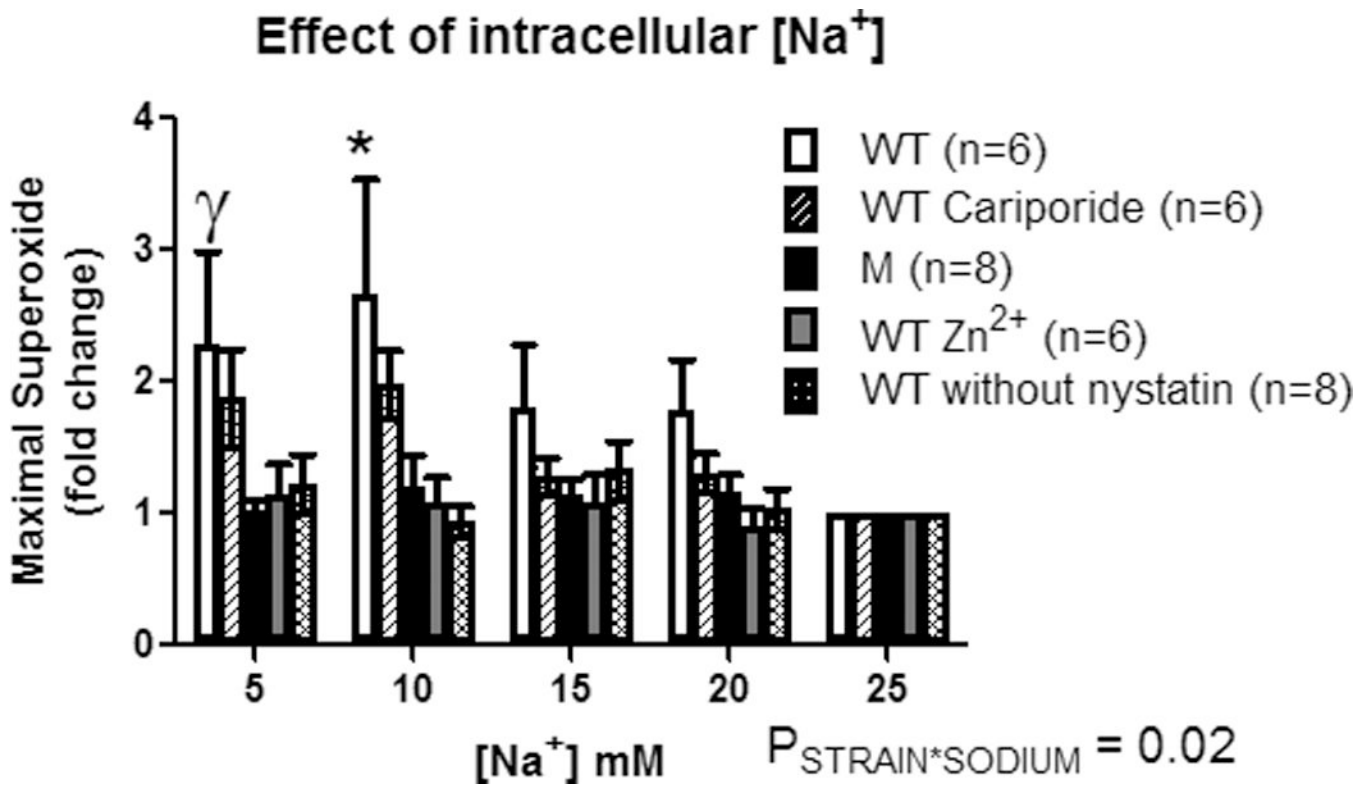


**Figure 4. Effect of intracellular $Na^+$ concentration on the respiratory burst in macrophages**

X-axis, intracellular $Na^+$ concentration ($[Na^+]_I$). Y-axis, maximal superoxide production in freshly isolated peritoneal rat macrophages following addition of PMA (100mM) determined by L-012 luminescence (data normalized to the response at 25mM $[Na^+]_I$ within each animal). Wild-type (open columns; n=6); Wild-type + 100μM cariporide (hatched columns; n=6); HV1 mutant (closed columns; n=8); Wild-type + 100μM $ZnCl_2$ (grey filled columns; n=6); Wild-type without addition of Nystatin (double hatched columns; n=8). Data were compared using 2-way ANOVA with Bonferroni post-hoc test comparing Wild-type to all other groups. * = $p<0.05$ comparing Wild-type to HV1 mutant, Wild-type + $ZnCl_2$ and Wild-type without Nystatin. Y = $p<0.05$ comparing Wild-type to HV1 mutant only. Data are mean±SE.

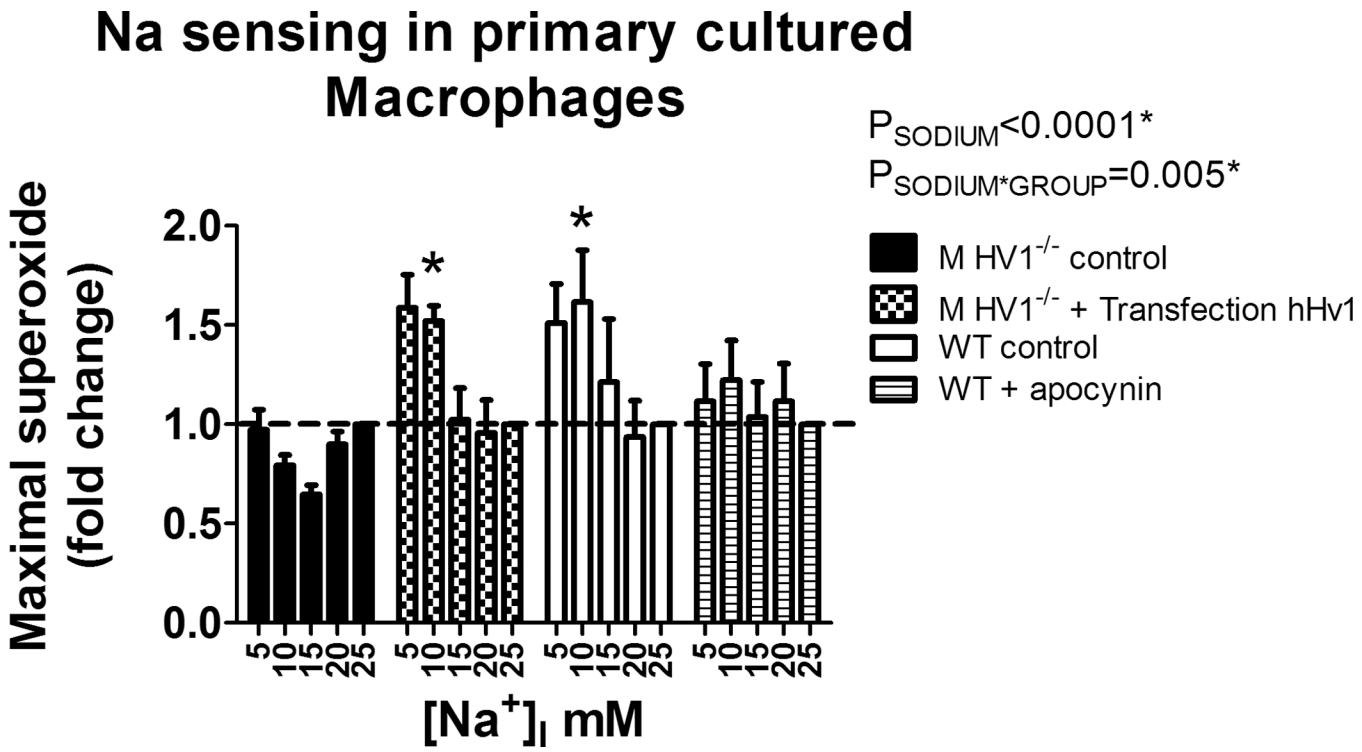


**Figure 5. Contribution of Hv1 and NAD(P)H oxidase toward Na sensing in primary cultured macrophages**

X-axis, intracellular Na+ concentration ([Na+]I). Y-axis, maximal superoxide production in freshly isolated peritoneal rat macrophages following addition of PMA (100mM) determined by L-012 luminescence (data normalized to the response at 25mM [Na+]I within each animal). $HV1^{-/-}$ control (closed columns; n=5); Wild-type (WT) control (open columns; n=5); Wild-type + apocynin 100μM (striped columns; n=5); $HV1^{-/-}$ transfected with human Hv1 (checked columns; n=5). Data were compared using 2-way ANOVA with Bonferroni post-hoc test comparing $HV1^{-/-}$ control to all other groups. * = $p<0.05$. Data are mean±SE.

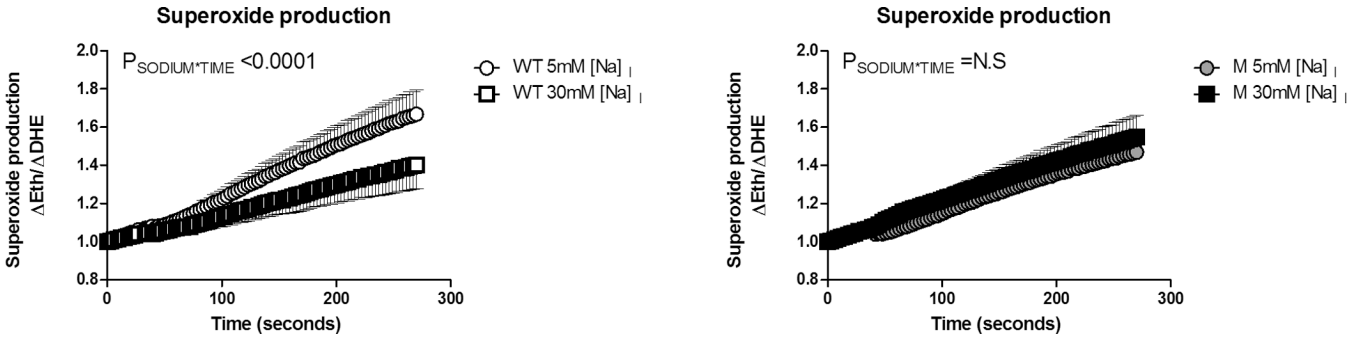


**Figure 6. Superoxide production in response to $H^+$ efflux at low and high intracellular $Na^+$ in mTAL**

Superoxide production in isolated medullary thick ascending limb from wild-type (WT; left panel; n=6) and $HV1^{-/-}$ mutant (M; right panel; n=7) rats loaded with the superoxide sensitive dye, dihydrethidium. Open circles, wild type at 5mM intracellular [$Na^+$]; open squares, wild type at 30mM intracellular [$Na^+$]; closed circles, mutant at 5mM intracellular [$Na^+$]; grey filled squares, mutant at 30mM intracellular [$Na^+$]. × axis, time in seconds. $NH_4Cl$ (20mM) was removed from the bath at t=30 seconds. Y axis, superoxide production (ΔEth/ΔDHE) normalized to 1 at t=0. $P_{SODIUM*TIME}$, result of a two-way repeated measures ANOVA comparing response within strain at 5 and 30mM intracellular [$Na^+$]. N.S = not significant. Data are mean±SE.

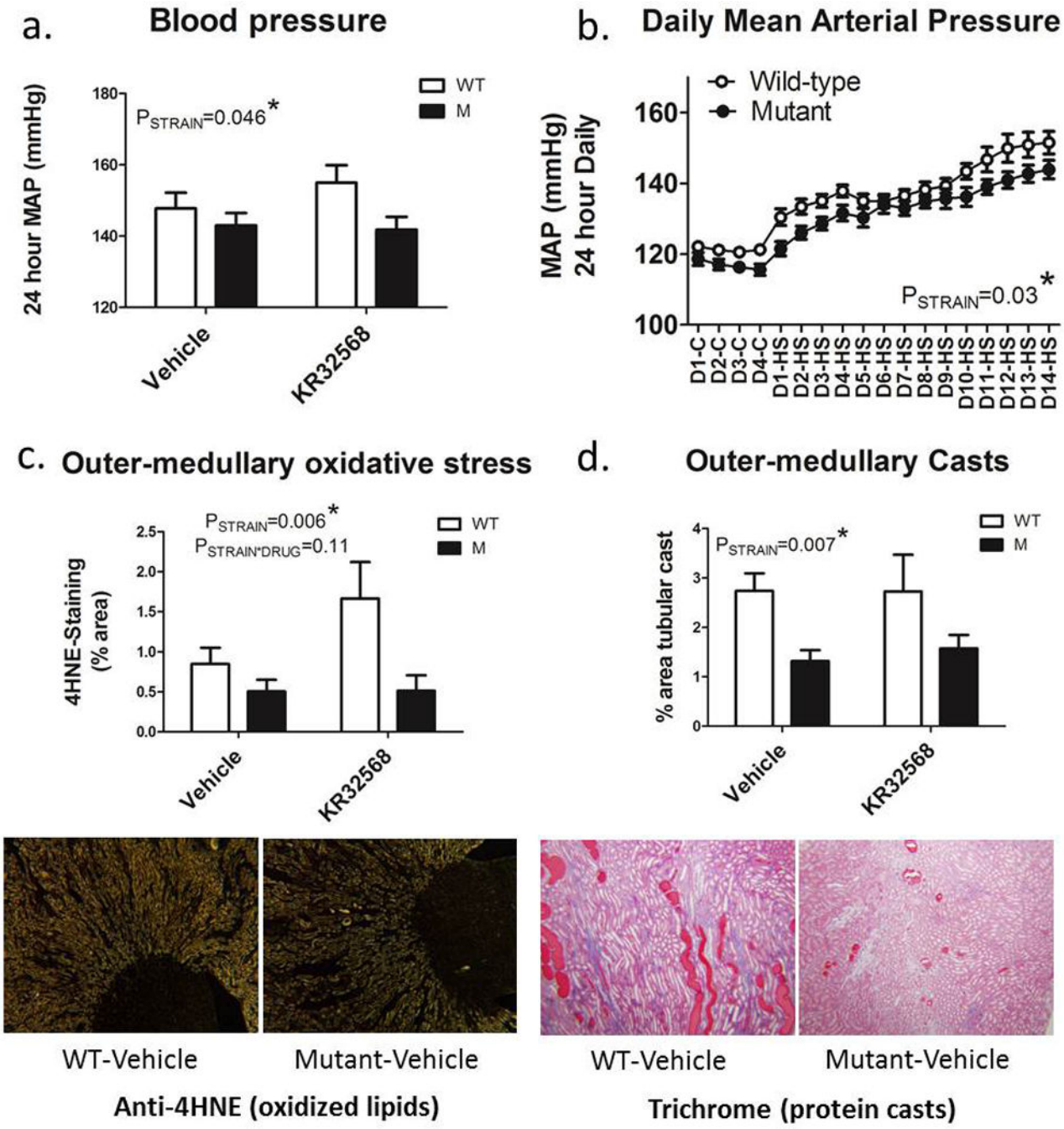


**Figure 7. Blood pressure, renal outer-medullary oxidative stress and tubulointerstitial injury in wild-type and HV1 mutant Dahl salt-sensitive rats**

**a**) average 24 hour mean arterial pressure as measured by radio-telemetry over the final 3 days of high (8%) NaCl feeding for two weeks in wild-type (WT; open columns) and $HV1^{-/-}$ mutant (M; closed columns) maintained on either vehicle (right) or given the NHE-1 inhibitor KR32568 (2mg/kg/day) from day 4 of high salt feeding (left). **b**) 24 hour daily mean arterial blood pressures (mmHg) as measured by radio-telemetry during 0.4% NaCl control (C) and 8% high salt (HS) feeding for 14 days (D). Open circles, wild type

(n=12); closed circles, $HV1^{-/-}$ mutant (n=12). All animals received only vehicle infusions until day 3 of high salt feeding (D3-HS). Drug or vehicle infusions were maintained until day 14 of high salt feeding (D14-HS). **c**) outer-medullary oxidative stress as determined by anti-4-HNE staining of the outer-medullary region. Shown are representative images of anti-4HNE staining in the outer-medulla and papilla of vehicle treated wild-type (left) and $HV1^{-/-}$ mutant rats (right) demonstrating more intense membrane staining of mTAL in wild-type animals. **d**) outer-medullary protein casts (% outer-medullary area). Shown are representative trichrome stained images of the outer-medulla vehicle treated wild-type (left) and $HV1^{-/-}$ mutant rats (right) demonstrating greater % area containing of brightly colored protein casts in wild-type animals. All histological measurements were assessed at the end of the study after 14 days of high salt feeding. Data are mean±SE. All data were compared with 2-way ANOVA.